

# The shadow and photon sphere of the charged black hole in Rastall gravity

Sen Guo<sup>\*1</sup>, Ke-Jian He<sup>2</sup>, Guan-Ru Li<sup>1</sup>, Guo-Ping Li<sup>\*3</sup>

<sup>1</sup>Guangxi Key Laboratory for Relativistic Astrophysics, School of Physical Science and Technology, Guangxi University, Nanning 530004, People's Republic of China

<sup>2</sup>College of Physics, Chongqing University, Chongqing 401331, People's Republic of China

<sup>3</sup>Physics and Space Science College, China West Normal University, Nanchong 637000, People's Republic of China

E-mail: sguophys@126.com; gpliphys@yeah.net

June 2021

**Abstract.** Considering a charged black hole (BH) surrounded by a perfect fluid radiation field (PFRF) in Rastall gravity, we investigate this BH shadow and photon sphere on different spherical accretions backgrounds. The effect of the PFRF parameter/BH charge on the critical impact parameter is studied by investigating the light deflection near this BH. The luminosity of these BH shadows in different spherical accretions is obtained, respectively. It is found that the shadow of this BH with infalling spherical accretion is darker than static spherical accretion, and the photon sphere with infalling spherical accretion is brighter than a static one. We creatively investigate the effects of the BH charge/PFRF parameter on the luminosity of BH shadow and photon sphere. The results implying that the BH shadow is a signature of space-time geometry, and the photon sphere luminosity is affected by accretion materials and BH itself.

*Keywords:* Black hole shadow, Photon sphere, Spherical accretion

## 1. Introduction

Black hole (BH) is one of the most interesting predictions in general relativity. The gravitational wave detection result is the first strong evidence for BH existence in the universe [1]. The stronger evidence is *M87\** image from the Event Horizon Telescope [2]. The light ray from the universe's accretion materials is received by BH's strong gravity field, which produces a marked deficit of the observed intensity inside the apparent boundary. It is the BH shadow. Furthermore, the light ray bend causes the BH to be surrounded by shadow and make the photon sphere produces luminosity [3]. Synge discovered the spherical BH shadow outline as a standard circle for the first time in 1966 [4]. Bardeen calculated the Schwarzschild BH shadow radius is  $r_s \equiv 5.2M$  [5].

More researches on BH shadow appears in [6–20], which shows that the gravity drag of the null geodesics line cause BH shadow shape change.

Apart from the study of shadow shape, the BH properties with different accretion materials have been investigated. Zeng *et.al* found that the Gauss-Bonnet coefficient affects the Gauss-Bonnet BH shadow [21]. The quintessence dark energy's contribution to BH shadow and photon ring was discussed in [22]. By investigating disk accretion material, Wald *et.al* obtained the relationship between BH shadow, photon rings, and lensing rings [23]. Inspired by these researches, the luminosity of BH shadow and photon sphere on various spherical accretions backgrounds has aroused our attention. That is one of the motives in this paper.

BH shadow research allows us to comprehend the BH's configuration but also help us exploring various gravity model more deeply. By investigating the charged rotating regular BHs shadow cast, Kumar *et.al* found that BH angular momentum leads to BH shadow no longer a standard circle [24]. Using the WKB approach and time-domain integration method, Konoplya *et.al* discussed the quasinormal modes and grey-body factors with different spin and shadow cast of the quantum correction Schwarzschild solution. The results show that the radius of the shadow is decreasing when the quantum deformation is turned on [25]. Övgün *et.al* obtained the visibility of a spherically symmetric non-commutative BH shadow depends on the non-commutative parameter in Rastall gravity [26]. Then, the BH shadows characteristics have been extensively discussed on the various gravity backgrounds [27–31] *etc.*

In another respect, Rastall proposed an extended theory of general relativity in 1972 [32]. Because the current experiment cannot be sure that the derivative of energy-momentum tensor is zero in the curved space-time, Rastall thought that the equivalence principle in general relativity is stringent, who proposed the Einstein field equation is modified as  $G_{\mu\nu} + \kappa\lambda g_{\mu\nu}R = \kappa T_{\mu\nu}$ , the  $\lambda$  is the Rastall parameter, and  $\kappa \equiv 8\pi G_N/c^4$  is the proportional constant in Einstein field equation that connects Einstein tensor with energy-momentum tensor [32]. Interestingly, by identifying that this modified energy-momentum tensor is a physical one, Visser considers that Rastall gravity is equivalent to Einstein gravity, which is beneficial for us to have a deeper understanding of Rastall gravity [33]. Then, Heydarzade *et.al* investigated solutions of BH surrounded by perfect fluid in Rastall theory [34], and Pourhassan *et.al* obtained the thermodynamics of these BH solutions [35].

Nevertheless, the shadow and photon sphere of the charged BH surrounded by PFRF in Rastall theory contexts research is still of opening question. This paper focuses on this issue. We focus primarily on the simple case of emission from an optically and geometrically thin spherical accretion near this BH. Considering the static and infalling spherical accretions, we analyze this BH shadow and photon sphere with spherical accretions and further investigate the influence of BH parameters on their luminosity.

The organization of this work is as follows. In Section 2, a charged BH surrounded by PFRF in Rastall theory is considered, and we investigate the light deflection near this BH. In Section 3, we study the shadow and photon sphere of this BH in various spherical

accretions. We draw the conclusions and discussions in Section 4. For simplicity, we adopt the units  $G_N = \hbar = \kappa_B = c = 1$ .

## 2. The charged BH surrounded by PFRF in Rastall gravity and light deflection

Considering a charged BH surrounded by PFRF in Rastall theory, the BH metric is given by [34]

$$ds^2 = -f(r)dt^2 + \frac{dr^2}{f(r)} + r^2 d\Omega^2, \quad (1)$$

where BH metric potential can be written as

$$f(r) = 1 - \frac{2M}{r} + \frac{4\pi G_N(Q^2 - N_r)}{c^4 r^2}, \quad (2)$$

in which  $M$  is BH mass,  $Q$  is BH charge, and  $N_r$  is the radiation field (RF) parameter. We found that this metric potential is similar to the Reissner-Nordström (RN) BH with an effective charge  $Q_{eff} = \sqrt{Q^2 - N_r}$ . Compared to the RN BH, the appearance of effective charge in the BH solution non-change the causal structure and Penrose diagrams of this BH solution. Taking the natural unit, the charged BH surrounded by PFRF in Rastall gravity horizon radius is obtained, i.e.

$$r_{\pm}^P = M \pm \sqrt{M^2 - Q^2 + N_r}, \quad (3)$$

where  $r_{\pm}^P$  represents event horizon radius ( $r_+^P$ ) and inner horizon radius ( $r_-^P$ ), respectively. Compared with the horizon radius of RN BH, our BH contain RF parameter term, this result is interpreted as the positive contribution of the RF characteristic to BH effective charge.

Next, we reviewed the deflection of photons. Due to the interaction between light ray and BH gravity field, the light rays deflect when it passes from the BH vicinity. The motion of light rays satisfies the Euler-Lagrangian equation in space-time. We have

$$\frac{d}{d\zeta} \left( \frac{\partial \mathcal{L}}{\partial \dot{x}^\alpha} \right) = \frac{\partial \mathcal{L}}{\partial x^\alpha}, \quad (4)$$

where  $\zeta$  is an affine parameter,  $\dot{x}^\alpha$  is the four-velocity of photon. The Lagrangian  $\mathcal{L}$  including the zero geodesics as following

$$\mathcal{L} = -\frac{1}{2} g_{\alpha\beta} \dot{x}^\alpha \dot{x}^\beta = \frac{1}{2} \left( f(r) \dot{t}^2 - \frac{\dot{r}^2}{f(r)} - r^2 \dot{\theta}^2 - r^2 \sin^2 \theta \dot{\varphi}^2 \right). \quad (5)$$

Because of the symmetry, it suffices to consider geodesics in the equatorial plane, i.e.  $\theta_0 = \pi/2$ ,  $\dot{\theta}_0 = 0$ , and  $\ddot{\theta}_0 = 0$ . According to equations (2) and (5), BH metric is static spherically symmetric, which implies that it is a non-function of time  $t$  and angle  $\varphi$ , satisfying  $(\partial \mathcal{L} / \partial t) = 0$  and  $(\partial \mathcal{L} / \partial \varphi) = 0$ . Therefore, there is a pair of conserved quantities of energy and angular momentum

$$E = \left( \frac{\partial \mathcal{L}}{\partial \dot{t}} \right) = f(r) \frac{dt}{d\zeta}, \quad L = - \left( \frac{\partial \mathcal{L}}{\partial \dot{\varphi}} \right) = r^2 \frac{d\varphi}{d\zeta}. \quad (6)$$

The four-velocity of time, azimuthal, and radial components satisfy the motion equation,

$$\left(\frac{dt}{d\zeta}\right) = \frac{L}{bf(r)}, \quad \left(\frac{d\varphi}{d\zeta}\right) = \pm \frac{L}{r^2}, \quad \left(\frac{dr}{d\zeta}\right)^2 + \frac{f(r)}{r^2} = \frac{1}{b^2}, \quad (7)$$

where  $b$  is defined as impact parameter ( $b \equiv |L|/E$ ) and  $\pm$  corresponding to the light rays motion counterclockwise and clockwise direction, respectively. Considering the null geodesic  $\mathcal{L} = 0$ , the orbit equation ( $\dot{r}^2/\dot{\varphi}^2$ ) for lightlike geodesics is obtained. Hence, the effective potential of the charged BH surrounded by PFRF in Rastall gravity can be written as

$$V_{eff} = \frac{f(r)}{r^2} = \frac{1}{r^2} \left(1 - \frac{2M}{r} + \frac{Q^2 - N_r}{r^2}\right). \quad (8)$$

The photon sphere orbit conditions are  $\dot{r} = 0$  and  $\ddot{r} = 0$ , the effective potential should satisfy the conditions

$$V_{eff} = \frac{1}{b^2}, \quad V'_{eff} = 0. \quad (9)$$

Based on equation (9), the numerical results of the event horizon radius  $r_+^P$  of this BH, the shadow radius  $r_{sh}^P$ , and impact parameter  $b_{ph}$  of photon sphere for different values of BH charges/RF parameters have been given in Table 1 and Table 2. We can see that  $r_+^P$ ,  $r_{sh}^P$  and  $b_{ph}$  are all smaller and smaller with the increase of the BH charge when  $N_r$  is given. Moreover, the parameter  $N_r$  has the opposite effect. It is worth mentioning that we adopt the natural unit system for simplicity, thus giving the pure number solution in tables.

**Table 1.** The event horizon, shadow radius and impact parameter for different  $Q$  with  $M = 1$  and  $N_r = 1$ .

Q	0.2	0.4	0.55	0.7	0.85	0.9
$r_+^P$	2.4	2.35647	2.30288	2.22882	2.13027	2.09087
$r_{sh}^P$	3.54206	3.48242	3.40919	3.30831	3.17481	3.12173
$b_{ph}$	5.91297	5.8331	5.7353	5.60116	5.42477	5.35504

**Table 2.** The event horizon, shadow radius and impact parameter for different  $N_r$  with  $M = 1$  and  $Q = 0.6$ .

RF	1	2	3	4	5.5	7
$r_+^P$	2.28062	2.62481	2.90788	3.37487	3.4779	3.76405
$r_{sh}^P$	3.378832	3.8516	4.24408	4.89559	5.03977	5.44081
$b_{ph}$	5.69486	6.33041	6.86507	7.76132	7.96073	8.51686

We plot the effective potential as a function of  $r$  for different BH charges/RF parameters in figure 1. It is evident that the radius and critical impact parameters decrease with an increase in BH charge for a given RF parameter. In contrast, the RF parameter has the opposite effect when the BH charge is fixed.

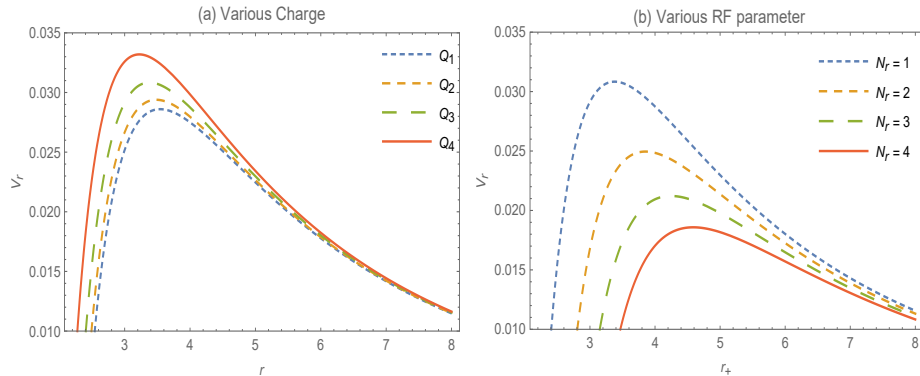


**Fig 1.** Effective potential  $V(r)_{eff}$  as a function of radius  $r$ . *Panel (a)* – Various charges  $Q = 0.2, 0.4, 0.6, 0.8$  with  $N_r = 1, M = 1$  and *Panel (b)* – Various RF parameters  $N_r = 1, 2, 3, 4$  with  $Q = 0.6, M = 1$ .

By introducing a new parameter  $u \equiv 1/r$  and according to equation (7), we have

$$\frac{du}{d\varphi} = \sqrt{\frac{1}{b^2} - u^2(1 - 2Mu - N_r u^2 + u^2 Q^2)} \equiv \Omega(u). \quad (10)$$

Assuming that all the light rays from accretions approach the BH from the right side, the BH produces shadow as the light is deflected. By using the ray-tracing code [36] and equation (10), the light ray trajectory is shown in figure 2.

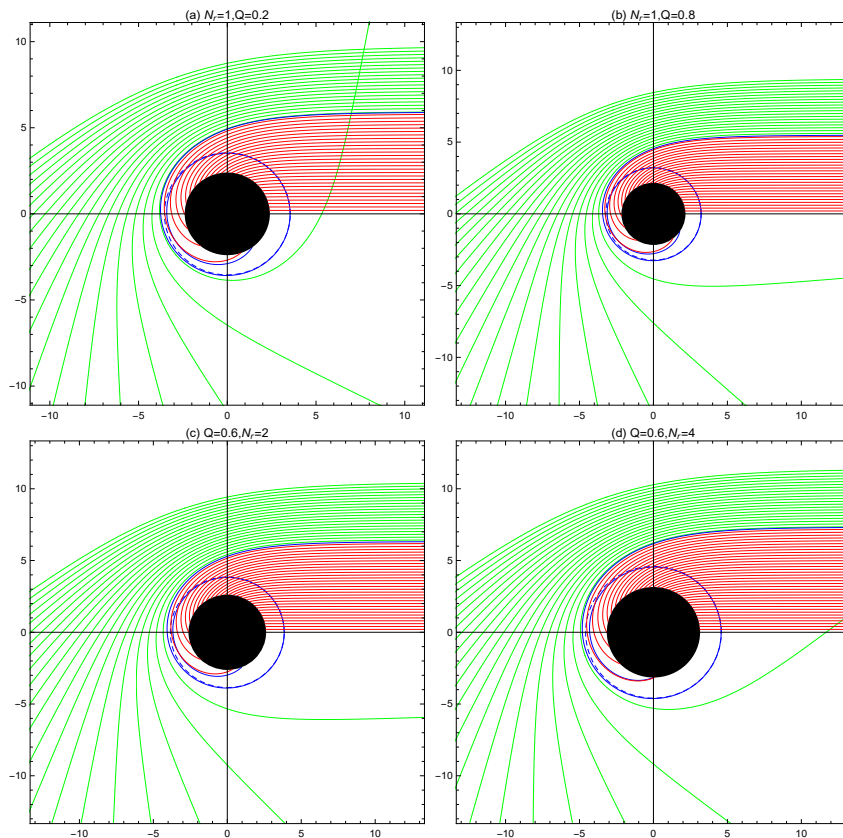


**Fig 2.** *Panel (a, b)* – Various charges  $Q = 0.2, 0.8$  with  $N_r = 1, M = 1$ . and *Panel (c, d)* – Various RF parameters  $N_r = 2, 4$  with  $Q = 0.6, M = 1$ . The green lines, blue lines and red lines correspond to  $b > b_{ph}$ ,  $b = b_{ph}$  and  $b < b_{ph}$ , respectively. The BH is shown as a solid disk and photon orbit as a dashed blue line.

In figure 2, it is evident that this BH shadow radius  $r_{sh}^P$  decreases when the BH charge increases. In comparison, the BH shadow radius increases with an increase in the RF parameter for given BH charge, which is consistent with the cases in table 1 and table 2. Compare the results of figure 2–(a) and (b), we found that the deflection of a light ray at the shadow is smaller, and the light ray density is lower when the value of  $q$  is larger. By comparing figure 2–(c) and (d), the deflect light ray at the shadow is larger, and the light ray density is higher when the value of  $N_r$  is larger.

### 3. BH shadow and photon sphere on different spherical accretions

#### 3.1. The static spherical accretion

Considering static spherical accretion for the thin of optically and geometrically. The intensity of radiation  $I(v_{obs})$  coming to a far observer at the frequency  $v_{obs}$  along any ray is given by [37, 38]

$$I(v_{obs}) = \int_{ray} g^3 j(v_{em}) dl_{prop}, \quad (11)$$

where  $g \equiv v_{obs}/v_{em}$  is gravity redshift factor,  $v_{em}$  is emitter photon frequency,  $j(v_{em})$  is emissivity per unit volume, and  $dl_{prop}$  is proper length differential as measured in the frame comoving with the matter. By assuming monochromatic with rest-frame frequency  $v_t$ , the proper length measured in the rest frame of emitter for BH is obtained, i.e.

$$g = f(r)^{1/2}, \quad j(v_{em}) \propto \frac{\delta(v_{em} - v_t)}{r^2}, \quad dl_{prop} = \sqrt{f(r)^{-1} + r^2 \left(\frac{d\varphi}{dr}\right)^2} dr. \quad (12)$$

According to equations (11) and (12), the specific intensity observed  $I(v_{obs})$  by the distant observer can be re-written as

$$I(v_{obs}) = \int_{ray} \frac{f(r)^{3/2}}{r^2} \sqrt{f(r)^{-1} + r^2 \left(\frac{d\varphi}{dr}\right)^2} dr. \quad (13)$$

Based on equations (2) and (13), the luminosity of this BH shadow and photon sphere on static spherical accretion background for a distant observer is obtained. We plot specific intensity  $I(v_{obs})$  as a function of impact parameter  $b$  for different RF parameters and BH charges in figure 3, respectively. We can see that  $I(v_{obs})$  reaches a peak rapidly with the increased impact parameter and decreases gradually to a minimum value. Because the light rotates around BH many times in photon sphere orbit, the optical path is infinite, and the resulting  $I(v_{obs})$  is the strongest at  $b_{ph}$ . In addition, the peak value of intensity increase with an increase of BH charge when the RF parameter is a constant, but  $b$  corresponding to the peak value decreases with an increase of BH charge. The result is consistent with the results in table 1. The RF parameter has the opposite effect when the BH charge is fixed.

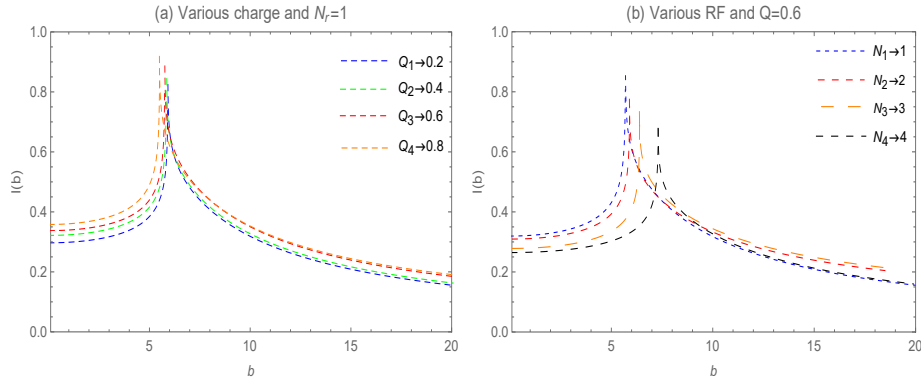


**Fig 3.** Profiles of intensity  $I(b)$  with static spherical accretion. *Panel (a)* – Various charges  $Q = 0.2, 0.4, 0.6, 0.8$  with  $N_r = 1, M = 1$  and *Panel (b)* – Various RF parameters  $N_r = 1, 2, 3, 4$  with  $Q = 0.6, M = 1$ .

Furthermore, the shadow cast by this BH in the  $(x, y)$  plane is shown in figure 4. We can see that the photon sphere with the strongest luminosity is outside of the BH shadow, and the inner region of the shadow is not entirely black. Because of the radiation field existence, the tiny fraction of photons escape from BH, and the photon sphere luminosity becomes more prominent with the enhancement of the RF parameter. Moreover, the maximum luminosity of the shadow image is attenuated with the increase of the BH charge when the RF parameter is fixed.

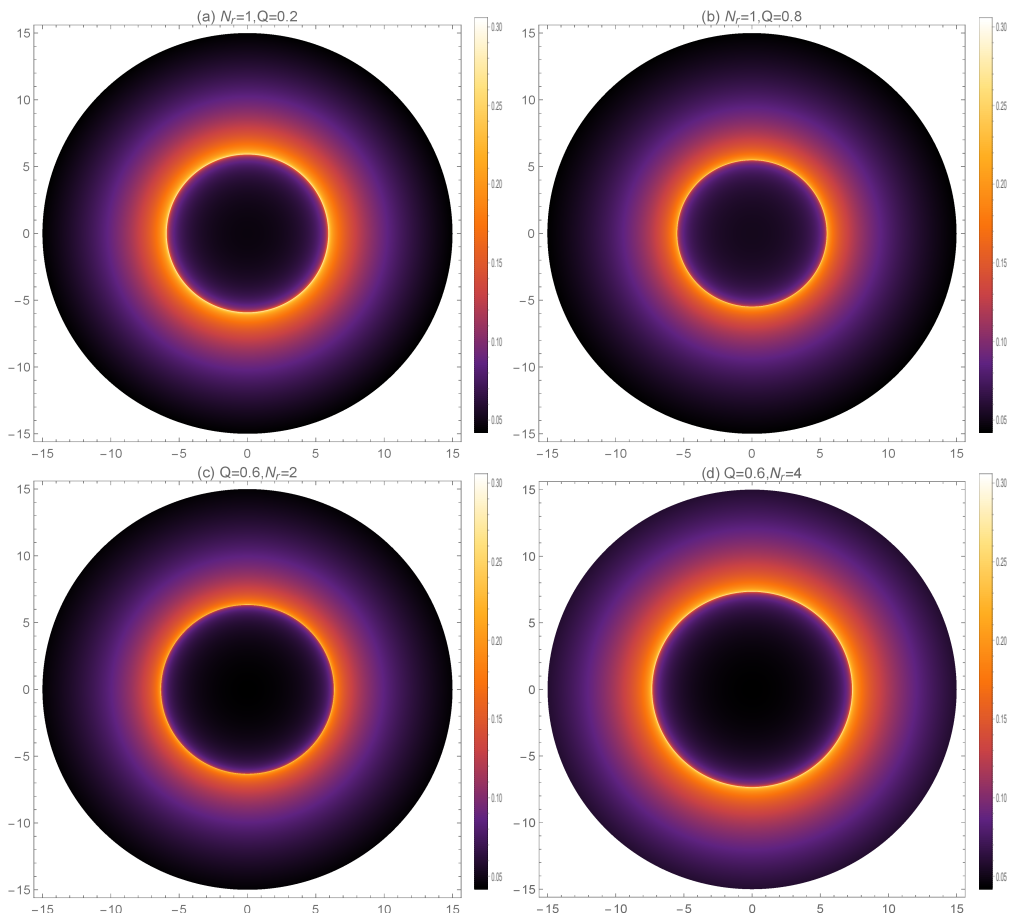


**Fig 4.** BH shadows and photon spheres cast with static spherical accretion in the  $(x, y)$  plane. *Panel (a, b)* – Various charges  $Q = 0.2, 0.8$  with  $N_r = 1, M = 1$  and *Panel (c, d)* – Various RF parameters  $N_r = 2, 4$  with  $Q = 0.6, M = 1$ .

### 3.2. The infalling spherical accretion

As we all know, most accretions are moving in the universe. This section considers BH shadow and photon sphere on infalling spherical accretion background, which is more accurate than static spherical accretion. Assuming that infalling spherical accretion falling onto BH from infinity, equation (13) is still determined to be effective. The redshift factor, in this case, is different from static spherical accretion. It is

$$g = \frac{k_\alpha u_{obs}^\alpha}{k_\vartheta u_{em}^\vartheta}, \quad (14)$$

where  $k^\mu \equiv \dot{x}_\mu$ ,  $u_{obs}^\mu \equiv (1, 0, 0, 0)$ ,  $u_{em}^\mu$  corresponding to photon four-velocity, distant observer four-velocity and accretion four-velocity, respectively. According to equation (7), one can get  $k_t$  is a constant ( $1/b$ ), and  $k_r$  comes from  $k_\vartheta k^\vartheta = 0$ , hence, we have

$$\frac{k_r}{k_t} = \pm \frac{1}{f(r)} \sqrt{1 - \frac{b^2 f(r)}{r^2}}, \quad (15)$$

where the sign here indicates that photons are approaching or away from BH. The accretion under consideration four-velocity as

$$u_{em}^t = \frac{1}{f(r)}, \quad u_{em}^\theta = u_{em}^\varphi = 0, \quad u_{em}^r = -\sqrt{1 - f(r)}. \quad (16)$$

According to above equations, the redshift factor of infalling spherical accretion can be written as

$$g_f = \frac{1}{u_{em}^t + k_r/k_{em} u_{em}^r}, \quad (17)$$

and the proper distance as

$$dl_{prop} = k_\vartheta u_{em}^\vartheta d\zeta = \frac{k_t}{g_f |k_r|} dr. \quad (18)$$

Therefore, the specific intensity  $I(v_{obs})$  with infalling spherical accretion can be rewritten as

$$I_f(v_{obs}) \propto \int_{ray} \frac{g_f^3 k_t dr}{r^2 |k_r|}. \quad (19)$$

Similar to static spherical accretion, the specific intensity with infalling spherical accretion  $I_f(v_{obs})$  also reaching a peak rapidly with the increased impact parameter and finally decreases gradually to a minimum value. For different RF parameters/BH charges, the numerical results of  $I_f(v_{obs})$  are plotted in figure 5. Comparing figure 3 shows that the specific intensity shape of infalling spherical accretion is similar to static spherical accretion. Nevertheless, the infalling spherical accretion has a sharp rise before reaching the peak, which means that the photons are quickly captured by BH and resulting in a halo when the impact parameter reaches  $b_{ph}$ .



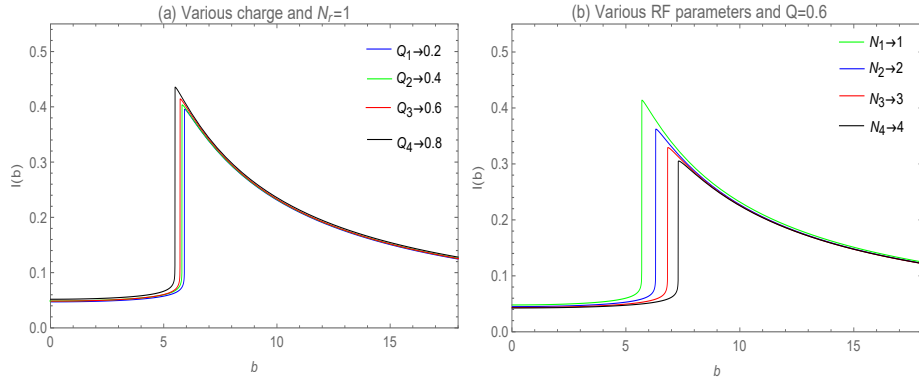


**Fig 5.** Profiles of intensity  $I(b)$  with infalling spherical accretion. *Panel (a)* – Various charges  $Q = 0.2, 0.4, 0.6, 0.8$  with  $N_r = 1, M = 1$  and *Panel (b)* – Various RF parameters  $N_r = 1, 2, 3, 4$  with  $Q = 0.6, M = 1$ .

We also plot the BH shadow cast with infalling spherical accretion in figure 6. It is shown that the BH shadow size in infalling spherical accretion background is mainly affected by the RF parameter. The larger the RF parameter is, the larger radius of BH shadow will be. For the luminosity of the photon sphere, the more significant BH charge is, the photon sphere luminosity will be darker when the RF parameter is constant. While the BH charge is a constant, the luminosity of the photon sphere faintly increases gradually with the increase of the RF parameter.

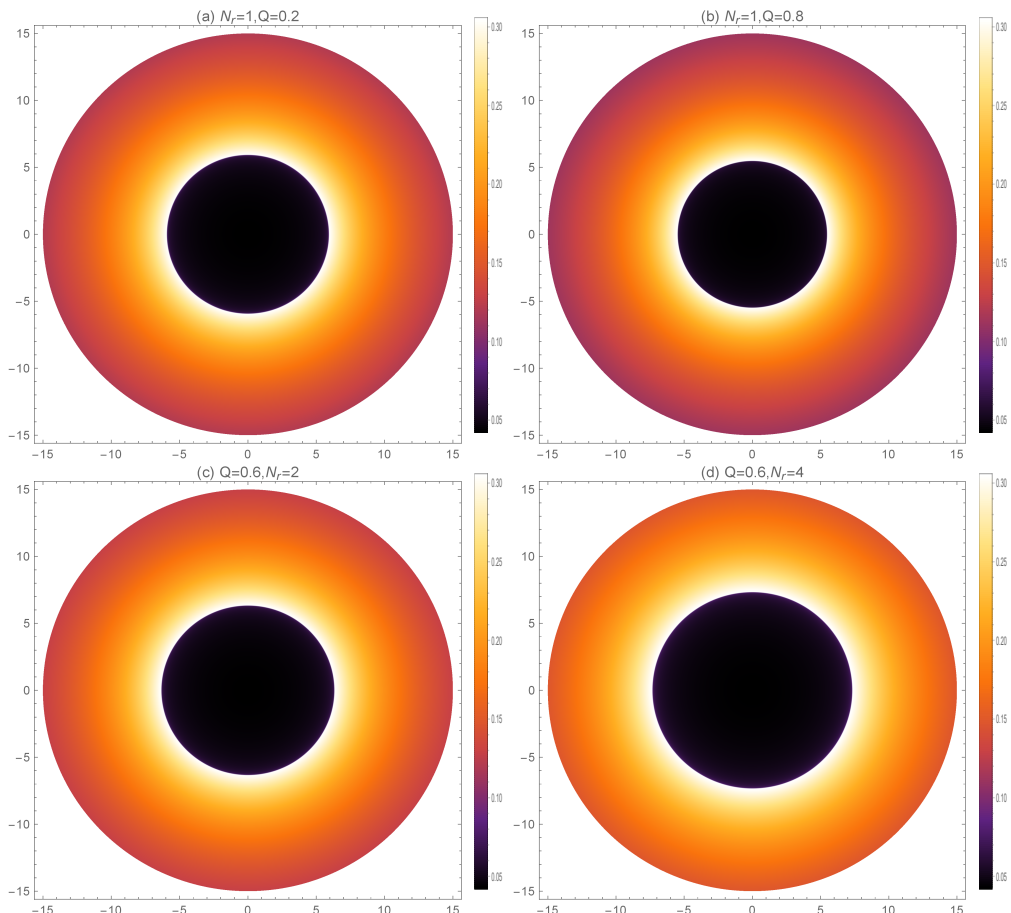


**Fig 6.** The BH shadows and photon spheres cast with infalling spherical accretion in  $(x,y)$  plane. *Panel (a, b)* – Various charges  $Q = 0.2, 0.8$  with  $N_r = 1, M = 1$  and *Panel (c, d)* – Various RF parameters  $N_r = 2, 4$  with  $Q = 0.6, M = 1$ .

#### 4. Conclusion

In this paper, the shadow and photon sphere of a charged BH surrounded by PFRF in Rastall gravity on different spherical accretions background is investigated, and further creatively analyse the effect of RF parameter/BH charge on BH shadow and photon sphere. We mainly discussed BH shadow size and photon sphere luminosity with static and infalling spherical accretions, respectively. When the BH charge is constant, the increase of RF parameter leads to the simultaneous increase of BH event horizon radius, shadow radius and critical impact parameter. The BH charge positively affects the effective potential, and the RF parameter harms the effective potential. As a result, the observers see the BH shadow of different sizes in various BH charges/RF parameters.

Then, we investigated the luminosity of BH shadow and photon sphere of this BH with static and infalling spherical accretions. We calculated the specific intensity observed by a distant observer and plotted the image of specific intensity as a function of impact parameter in various BH charges/RF parameters, which is shown that the peak value of intensity increase with BH charge increase when the RF parameter is a constant, but the  $b$  corresponding to the peak value decreases with an increase of BH charge. However, the RF parameter oppositely affects the critical impact parameter, and these are consistent with the results in table 1 and table 2.

This BH shadow and photon sphere cast in the  $(x, y)$  plane is shown in figure 4 and figure 6, showing that the shadow inner region is not entirely black. The photon sphere with the strongest luminosity is outside of BH shadow. The photon sphere image maximum luminosity is attenuated with an increase of BH charge when the RF parameter is fixed. The luminosity of the photon sphere faintly increases gradually with increased RF parameter for given the BH charge. Compared with the change of luminosity, the RF parameter has more influence on BH shadow size.

Compared with static and infalling spherical accretions, we obtain: *i)* the size and position of BH shadow and photon sphere non-change in case of static and infalling spherical accretions, which imply that BH shadow is a signature of space-time geometry; *ii)* BH shadow with infalling spherical accretion is darker than that of static spherical accretion in the central region, which means that most of the photons in static spherical accretion unit volume are captured by BH; *iii)* the photon sphere with infalling spherical accretion is brighter than a static one, showing a small number of photons accumulate in photon sphere for static spherical accretion; *v)* the increase of RF parameter has a positive effect on the photon sphere luminosity for different spherical accretions, while the effect of BH charge is opposite. The reason as the radiation field existence, the tiny fraction of photons escape from BH, and photon sphere luminosity becomes more prominent with the enhancement of RF parameter. On the other hand, the Hawking radiation suggests that BH with a more significant charge has a more substantial surface gravity  $\kappa$ , making photons easy to capture by BHs. From the point of view of spherical accretion, the impact parameter decreases with the increase in BH charge, which means that photons of light have more kinetic energy and make photons not easily captured

by BHs.

In our subsequent work, we will study the shadow and photon sphere of this black hole on the optically thin and geometrically thin/thick disk-shaped accretion background, and order to have a fuller understanding of the appearance of this black hole by investigating the photon rings and the lensing rings [39].

## Acknowledgments

The authors would like to thank the anonymous reviewers for their helpful comments and suggestions, which helped to improve the quality of this paper. This work is supported by the National Natural Science Foundation of China (Grant No.11903025).

## 5. References

- [1] B. Abbott et al., Observation of Gravitational Waves from a Binary Black Hole Merger, *Phys. Rev. Lett.* **116**: 061102 (2016).
- [2] K. Akiyama et al., First *M87* Event Horizon Telescope Results. I. The Shadow of the Supermassive Black Hole, *Astrophys. J.* **L1(6)**: 875 (2019).
- [3] P. V. P. Cunha and C. A. R. Herdeiro, Shadows and Strong Gravitational Lensing: A Brief Review, *Gen. Relativ. Grav.* **50**: 42 (2018).
- [4] J. L. Synge, The Escape of Photons from Gravitationally Intense Stars, *Mon. Not. R. Astron. Soc.* **131**: 463 (1966).
- [5] J. M. Bardeen, In Black holes, 215C239 (1973).
- [6] L. Amarilla, E. F. Eiroa and G. Giribet, Null geodesics and shadow of a rotating black hole in extended Chern-Simons modified gravity, *Phys. Rev. D.* **81**: 124045 (2010).
- [7] Z. L. Li, C. Bambi, Measuring the Kerr spin parameter of regular black holes from their shadow, *JCAP.* **1401**: 041 (2014).
- [8] A. Grenzebach, V. Perlick and C. Lmmerzuhl, Photon Regions and Shadows of Kerr-Newman-NUT Black Holes with a Cosmological Constant, *Phys. Rev. D.* **89**: 124004 (2014).
- [9] J. W. Moffat, Modified Gravity Black Holes and their Observable Shadows, *Eur. Phys. J. C.* **75**: 130 (2015).
- [10] V. Perlick, O. Y. Tsupko and G. S. B. Kogan, Influence of a plasma on the shadow of a spherically symmetric black hole, *Phys. Rev. D.* **92**: 104031 (2015).
- [11] M. Amir, S. G. Ghosh, Shapes of rotating nonsingular black hole shadows, *Phys. Rev. D.* **94**: 024054 (2016).
- [12] M. Sharif, S. Iftikhar, Shadow of a Charged Rotating Non-Commutative Black Hole, *Eur. Phys. J. C.* **76**: 630 (2016).
- [13] J. Grover, A. Wittig, Black Hole Shadows and Invariant Phase Space Structures, *Phys. Rev. D.* **96**: 024045 (2017).
- [14] N. Tsukamoto, Black hole shadow in an asymptotically-flat, stationary, and axisymmetric spacetime: The Kerr-Newman and rotating regular black holes, *Phys. Rev. D.* **97**: 064021 (2018).
- [15] Y. Mizuno, Z. Younsi, C. M. Fromm, et.al, The Current Ability to Test Theories of Gravity with Black Hole Shadows, *Nature Astronomy.* **2**: 585 (2018).
- [16] S. Haroon, M. Jamil, K. Jusufi, et.al, Shadow and Deflection Angle of Rotating Black Holes in Perfect Fluid Dark Matter with a Cosmological Constant, *Phys. Rev. D.* **99**: 044015 (2019).
- [17] R. A. Konoplya, T. Pappas, A. Zhidenko, Einstein-scalar-Gauss-Bonnet black holes: Analytical approximation for the metric and applications to calculations of shadows, *Phys. Rev. D.* **101**: 044064 (2020).
- [18] J. C. S. Neves, Upper bound on the GUP parameter using the black hole shadow, *Eur. Phys. J. C.* **80**: 343 (2016).
- [19] E. Contreras, . Rincn, ea.al, Black hole shadow of a rotating scale-dependent black hole, *Phys. Rev. D.* **101**: 064053 (2020).

- [20] K. Jusufi, Quasinormal Modes of Black Holes Surrounded by Dark Matter and Their Connection with the Shadow Radius, *Phys. Rev. D.* **101**: 084055 (2020).
- [21] X. X. Zeng, H. Q. Zhang and H. B. Zhang, Shadows and photon spheres with spherical accretions in the four-dimensional Gauss-Bonnet black hole, *Eur. Phys. J. C.* **80**: 872 (2020).
- [22] X. X. Zeng, H. Q. Zhang, Influence of quintessence dark energy on the shadow of black hole, *Eur. Phys. J. C.* **80**: 1058 (2020).
- [23] S. E. Gralla, D. E. Holz and R. M. Wald, Black Hole Shadows, Photon Rings, and Lensing Rings, *Phys. Rev. D.* **100**: 024018 (2019).
- [24] R. Kumar, S. G. Ghosh and A. Z. Wang, Shadow cast and deflection of light by charged rotating regular black holes, *Phys. Rev. D.* **100**: 124024 (2019).
- [25] R. A. Konoplya, Quantum corrected black holes: quasinormal modes, scattering, shadows, *Phys. Lett. B.* **804**: 135363 (2020).
- [26] A. Övgün, et.al, Shadow cast of non-commutative black holes in Rastall gravity, arXiv:1712.09793.
- [27] R. Kumar, S. G. Ghosh and A. Z. Wang, Gravitational deflection of light and shadow cast by rotating Kalb-Ramond black holes, *Phys. Rev. D.* **101**: 104001 (2020).
- [28] P. C. Li, M. Y. Guo and B. Chen, Shadow of a Spinning Black Hole in an Expanding Universe, *Phys. Rev. D.* **101**: 084041 (2020).
- [29] F. Ahmed, D. V. Singh and S. G. Ghosh, Five dimensional rotating regular black holes and shadow, arXiv: 2002.12031.
- [30] G. P. Li, K. J. He, Shadows and rings of the Kehagias-Sfetsos black hole surrounded by thin disk accretion, arXiv: 2105.08521.
- [31] K. J. He, S. Guo, S. C. Tan, G. P. Li, The feature of shadow images and observed luminosity of the Bardeen black hole surrounded by different accretions, arXiv: 2103.13664.
- [32] P. Rastall, Generalization of the Einstein Theory. *Phys. Rev. D.* **6**: 3357 (1972).
- [33] M. Visser, Rastall gravity is equivalent to Einstein gravity, *Phys. Lett. B.* **782**: 83 (2018).
- [34] Y. Heydarzade, F. Darabi, Black hole solutions surrounded by perfect fluid in Rastall theory, *Phys. Lett. B.* **771**: 365 (2017).
- [35] B. Pourhassan, S. Upadhyay, Thermal fluctuations of charged black hole solution in Rastall theory, arXiv:1910.11698.
- [36] R. Narayan, M. D. Johnson and C. F. Gammie, The Shadow of a Spherically Accreting Black Hole, *Astrophys. J.* **L33**: 885 (2019).
- [37] M. Jaroszynski and A. Kurpiewski, Optics near kerr black holes: spectra of advection dominated accretion flows, *Astron. Astrophys.* **326**: 419 (1997).
- [38] C. Bambi, Can the supermassive objects at the centers of galaxies be traversable wormholes? The first test of strong gravity for mm/sub-mm very long baseline interferometry facilities. *Phys. Rev. D.* **87**: 107501 (2013).
- [39] Sen. G, G. P Li, et.al, (to be published)